

Relativistic light-shift theory of few-electron systems: Heliumlike highly charged ionsO. Postavaru^{1,*} and A. C. Scafes^{2,†}¹*Faculty of Mathematics and Computer Science, University of Bucharest, Str. Academiei 14, 010014, Bucharest, Romania*²*Horia Hulubei National Institute of Physics and Nuclear Engineering, P.O. Box MG-6, 077125, Magurele, Romania*

(Received 13 January 2017; published 18 September 2017)

The light-shift theory of many-electron systems in a laser field is described using the projection operators technique. In heavy ions, the electrons are tightly bound by the Coulomb potential of the nucleus, which prohibits ionization even by strong lasers. However, interaction with the monofrequent laser field leads to dynamic shifts of the electronic energy levels, and the process is treated by second-order time-dependent perturbation theory. In order to treat heliumlike systems, one decomposes the corresponding matrix elements into hydrogenlike matrix elements using the independent particle model. We are applying a fully relativistic description of the electronic states by means of the Dirac equation. Our formalism goes beyond the Stark long-wavelength dipole approximation and takes into account nondipole effects of retardation and interaction with the magnetic field components of the laser beam.

DOI: [10.1103/PhysRevA.96.033412](https://doi.org/10.1103/PhysRevA.96.033412)**I. INTRODUCTION**

The dynamic light-shift (ac Stark shift) is a second-order perturbative effect [1] that shifts atomic energy levels in a laser field; ac Stark shift is quadratic in the field strength and can be understood as a time-averaged dc Stark shift [2,3]. It is the most important source of spectral line broadening and is an intrinsic undesirable effect in optical spectroscopy. A good experimentally determined absorption or fluorescence spectrum would show the ac Stark shift signature.

In the first part of this paper, we are focusing on the general presentation of the light-shift theory. It is an ordinary description of a n_e electron system in an electromagnetic field, which takes into account radiative corrections to the intermediate energies and the ionization rates. To solve this problem, we are using the so-called T -matrix formalism, a theory which is quite different to the common S -matrix expansion [4]. It has been applied to a wide range of processes, including dielectronic recombination [5,6] and resonance fluorescence [7]. The projection theorem [8] is the main tool we have used in order to solve our problem. In Fig. 1 is represented one of the situations that can occur in the light-ion interaction, technically speaking, one should sum over all possible bound intermediate states and integrate over all continuum ones.

Going beyond the electric-dipole approximation is important whenever studying electric-dipole-forbidden transitions, such as magnetic-dipole transitions, and in general, nondipolar effects become increasingly important when addressing higher-energy photons. We show that the magnetic contributions are insignificant, but the interaction operator allows us to include in our results the retardation effects, which are sizable in heavy ions.

In the second part of this paper we are studying heliumlike (He-like) systems in the independent particle model (IPM). In this model the electrons are assumed to move independently of each other in the average field generated by the nucleus and the other electrons.

The biggest advantage of working with He-like systems is their simple electronic structure, which gives us accurate results using standard theoretical methods, e.g., multiconfiguration Dirac-Fock or relativistic many-body perturbation theory. In contrast with the neutral atoms, in highly charged ions (HCI) the electron correlation effects are suppressed by a factor $1/Z$, which allows us to solve the problem perturbatively, to a high accuracy.

In order to test the standard model in the low-energy regime, parity nonconservation (PNC) effects using few-electron ions can provide new opportunities. There are many new and old theoretical investigations for PNC using HCI [9,10]. Heliumlike uranium seems to be the ideal candidate in order to observe interference effects between weak matrix elements and Stark matrix elements in two-photon $[1s2s]_{J=0} \rightarrow [1s2p_{1/2}]_{J=0}$ transitions in the high- Z domain [11]; we are expecting the off-resonant Stark-shift theory to have an important contribution to the experimental setup. This optical transition can be addressed experimentally by using, e.g., POLARIS-Jena [12]. Due to very significant progress in the x-ray laser development, e.g., PHELIX-GSI [13], now experimentalists can even induce transitions in the x-ray range for highly charged, heavy He-like ions.

The independent particle model allows us to decompose the He-like theory into the H-like theory, and the last one is known from literature (see, e.g., [14]). Computations are beyond dipole approximation, taking into account the retardation effect and the interaction with magnetic components of the laser field, allowing us to extend the field of investigations to stronger laser fields and higher frequencies. The level shifts calculated in the current article are important in experiments on the two-photon absorption of heliumlike ions planned at the GSI facility in Darmstadt and the Helmholtz Institute in Jena [15].

II. THEORY

The rigorous description of the HCI problem can be achieved only with quantum electrodynamics (QED). Different procedures have been developed during the last years to account for combined relativistic and QED effects as

*opostavaru@linuxmail.org†ascfases@tandem.nipne.ro

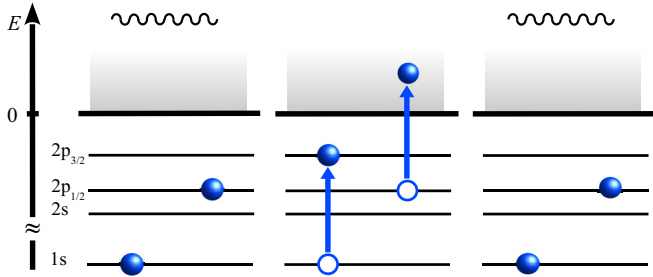


FIG. 1. The diagram schematically shows the two steps of the light-shift process (ion excitation-deexcitation in laser field). In the initial state, identical to the final one, the ion is in a bound state and a photon is present $|i\rangle = |q\rangle \otimes |1; \mathbf{k}\lambda\rangle$. The intermediate state $|d\rangle = \sum_q |q\rangle$ is a collection of all possible bound and continuous states.

well as electron correlations. One may distinguish between two classes of many-body approaches: variational and non-variational procedures. Schemes based on the variational principle were introduced a long time ago. In the multi-configuration Hartree-Fock (MCHF) and multiconfiguration Dirac-Fock (MCDF) methods one varies the orbitals and in the conventional self-consistent field (SCF) techniques, the mixing coefficients are varied, and the orbitals are kept fixed. The nonvariational method could be either perturbative or nonperturbative. The many-body perturbation theory (MBPT) is a frequently used scheme, based on diagrammatic technique. However, a closer analysis of these perturbative schemes reveals that application of expressions of higher order than fourth order for energies is more or less prohibited. In many problems one should go beyond that order, and this has led to various nonperturbative approaches such as the coupled cluster expansion (CCE).

The SCF and MBPT methods are by now also established in the relativistic framework. The resulting Hamiltonian is known as the Dirac-Coulomb Hamiltonian; however, its energy spectrum is not bounded from below with the consequence that eigenstates may dissolve into the negative energy continuum (continuum dissolution). Accordingly, this Hamiltonian does not represent a satisfactory basis for relativistic many-body calculations, and these difficulties can be avoided by performing a more rigorous and useful approximation based on the projected Dirac-Coulomb-Breit Hamiltonian, known as the no-virtual-pair approximation (NVPA), since virtual electron-positron pairs are explicitly excluded as intermediate states.

This also implies neglect of any radiative corrections (Lamb shift) up to this level of approximation. It is in fact a major challenge to be able to evaluate these energy shifts by *ab initio* methods. The potential approach is based on the derivation of effective electron-electron interaction potentials which, if incorporated in an iterative scheme, in principle accounts for the many-body and QED effects up to any desired accuracy [16]. The effective potential aligns two terms: the first term corresponds to the exchange of a single, virtual photon and can be specified to be the Coulomb-Breit interaction, and the second term corresponds to the irreducible part of the two-photon exchange that is not included by iterating the first part and possible higher-order photon-exchange diagrams.

For the QED description of the interelectron interaction in many-electron systems it is convenient to employ the Coulomb gauge. The general solution of the problem of how to account for the reducible graphs of S -matrix expansion actually implies the construction of the many-electron bound-state QED exact in all orders in nuclear charge Z (Furry picture) [17]. Unlike the case of light atoms, in heavy many-electron atoms the theoretical methods that avoid the use of $Z\alpha$ expansion become preferable (α is the fine-structure constant). Not only the innermost K -shell electrons, but also the valence (especially ns) electrons should be described exact to all orders in $Z\alpha$, since these electrons actually penetrate rather deeply into the electron core up to the regions where the screening is small and the effective charge Z_{eff} of the nucleus is nearly equal to the bare nuclear charge Z .

There is another rigorous QED perturbation theory approach which allows for exact QED description of ions based on the evaluation of the poles of the exact Green function for many-electron systems. The so-called two-time Green's function (TTGF) method [18] has proven to be a very powerful tool regarding higher-order QED calculations for the few-electron systems. Also, the adiabatic approach encounters problems with the treatment of degenerate states and with renormalization; such problems do not arise in TTGF.

The covariant evolution operator (CEO) approach [19] descends from the S -matrix approach, but it is similar to the two-time Green's function method in many features and possesses the same advantages. Instead of the S -matrix, the time-dependent evolution operator is employed as the main object within the covariant evolution operator approach. The CEO approach as well as the TTGF method allows for the QED calculations for the quasidegenerate states.

In this work, the atomic electrons are described within relativistic MBPT (RMBPT), but the electromagnetic field and its interaction with electrons are treated with the use of second quantization, i.e., within QED. We are developing a theory based on the T -matrix expansion instead of a standard QED perturbation theory. The T -matrix method is one of the most powerful and widely used theoretical techniques for the computation of electromagnetic scattering [20]. For application to processes involving multiple electron continua and multiple photon continua, it is advantageous to develop the T -matrix description by taking advantage of the projection-operator techniques (POT). POT allows us to present a general recipe for constructing matrix elements of the T operator for the light-shift effect for particular model systems of interest, featuring a limited number of discrete states and continua. We present an expression for T which separates naturally into two terms, one of which describes the direct radiative recombination process in the absence of autoionizing resonances, and the other which incorporates all effects of the autoionizing resonances (see Fig. 4).

The transition operator T is related to the scattering operator S by formula [21]

$$T = 1 - iS, \quad (1)$$

and provides a complete description of the light-shift process. The RMBPT follows as a direct generalization of the nonrelativistic MBPT, and like the QED theory, is a perturbative assumption. We note that for RMBPT one could

draw Feynman-like diagrams for the various terms in the infinite perturbation series.

In the relativistic many-body problem, the Dirac-Coulomb Hamiltonian encounters serious problems with continuum dissolution. The difficulties can be avoided by performing a useful approximation based on the projected Dirac-Coulomb-Breit Hamiltonian. As we have already mentioned, the radiative corrections are omitted within the NVPA. However, we know that Lamb shifts are quite significant in spectroscopic data for heavy ions, and it is a challenge to be able to evaluate these energy shifts by *ab initio* methods. A relativistic treatment of many-body interactions consistent to order $(Z\alpha)^2$ has been developed by using the frequency-independent part of the Coulomb-Breit interaction in the Coulomb gauge [16]. Beside the fact that using the Coulomb gauge one has to deal with complicated expressions for the effective potentials, there are certain inconveniences that arise from NVPA, such as problems with the treatment of degenerate states and renormalization.

To increase the precision and to solve the existent problems in literature, it becomes necessary to go beyond the standard NVPA scheme and to include retardation effects. In our model we are neglecting the first-order electron-electron interaction and applying the independent particle approximation, we are able to reduce the He-like problem to the H-like theory, which does not encounter any problem with the continuum dissolution. The theory is treated in the Babushkin gauge, taking into account the retardation effects. Another advantage presented by our model is that the radiative corrections are introduced by hand and the H-like Lamb shifts are well known [22].

A. Ion-laser interaction Hamiltonian

The Hamiltonian of a relativistic n_e -electron system in an electromagnetic field may be written as

$$\mathcal{H} = \mathcal{H}_e + \mathcal{H}_r + \mathcal{H}_{er}, \quad (2)$$

where the Hamiltonian \mathcal{H}_e is defined as [2,23]

$$\mathcal{H}_e = \sum_{i=1}^{n_e} h_i + \sum_{i<j}^{n_e} \frac{e^2}{4\pi\epsilon_0|\mathbf{r}_i - \mathbf{r}_j|} \quad (3)$$

and describes the Coulomb interaction between the electrons and the nucleus, together with the interaction between different electrons; the second term in Eq. (3) illustrates the Coulomb repulsion between electrons. The Hamiltonian h_i is representing the interaction of the i th electron with the nucleus and is given by the expression

$$h_i = c\boldsymbol{\alpha}_i \cdot \mathbf{p}_i + (\beta_i - 1)m_0c^2 + V_{\text{nuc};i}(r), \quad (4)$$

$$V_{\text{nuc};i}(r) = -\frac{Ze^2}{4\pi\epsilon_0|\mathbf{r}_i|},$$

where e is the elementary charge, ϵ_0 vacuum permittivity, m_0 electron mass, and c the speed of light. The 4×4 Dirac matrices $\boldsymbol{\alpha}_i$ and $\boldsymbol{\beta}$ have the representation [24]

$$\boldsymbol{\alpha}_i = \begin{pmatrix} 0 & \boldsymbol{\sigma}_i \\ \boldsymbol{\sigma}_i & 0 \end{pmatrix}, \quad \boldsymbol{\beta} = \begin{pmatrix} 1 & 0 \\ 0 & -1 \end{pmatrix}, \quad (5)$$

where $\boldsymbol{\sigma}_i$, $i \in \overline{1,3}$, are the 2×2 Pauli matrices.

The Hamiltonian of a free electromagnetic field is given in the second-quantized form as

$$\mathcal{H}_r = \sum_{\mathbf{k}} \sum_{\lambda=1}^2 \hbar\omega_{\mathbf{k}} a_{\mathbf{k}\lambda}^\dagger a_{\mathbf{k}\lambda}, \quad (6)$$

where $a_{\mathbf{k}\lambda}^\dagger$ and $a_{\mathbf{k}\lambda}$ are called the creation and the annihilation operators, respectively. An operator $a_{\mathbf{k}\lambda}^\dagger$ acting on the vacuum state is creating a photon with momentum \mathbf{k} and transverse polarization λ , ($\lambda \in \overline{1,2}$). \hbar is the reduced Planck constant.

The third term in Eq. (2) represents the interaction between the bound electrons and the radiation field,

$$\mathcal{H}_{er} = \sum_{i=1}^{n_e} \sum_{\mathbf{k}} \sum_{\lambda=1}^2 \sqrt{\frac{\hbar e^2 c^2}{2\epsilon_0 \omega_{\mathbf{k}} V}} \times \boldsymbol{\alpha}_i \cdot (\hat{\boldsymbol{\epsilon}}_{\mathbf{k}\lambda} e^{i\mathbf{k}\cdot\mathbf{r}_i} a_{\mathbf{k}\lambda} + \hat{\boldsymbol{\epsilon}}_{\mathbf{k}\lambda}^* e^{-i\mathbf{k}\cdot\mathbf{r}_i} a_{\mathbf{k}\lambda}^\dagger), \quad (7)$$

where $\hat{\boldsymbol{\epsilon}}_{\mathbf{k}\lambda}$ is the polarization vector of the photon field.

B. Projection operator technique

The light-shift is a two-step process (ion excitation-deexcitation in a laser field) in which are involved two different configuration types of many-particle states: the initial state, which is identical with the final one, is made up of a bound state and a photon, and the intermediate state contains only bound and continuous electrons in all possible configurations (see Fig. 1).

In order to treat the problem perturbatively, the total Hilbert space of states with n_e electrons and any number of photons is divided into several subspaces. This formalism, called Feshbach theory [25,26], is a consequence of the spectral theorem [27]. Let $\mathcal{Q}^{(n)}$ be the subspace containing the states with n photons and all electrons in bound states, and the subspace $\mathcal{P}^{(n)}$ the orthogonal complement of $\mathcal{Q}^{(n)}$ within the space of states with n photons; it includes those states in which at least one electron is found in a continuum. Since the subspaces defined here span the entire Hilbert space, the identity operator can be decomposed as [28]

$$1 = \sum_{n=0}^{\infty} (\mathcal{Q}^{(n)} + \mathcal{P}^{(n)}), \quad (8)$$

where $\mathcal{Q}^{(n)}$ and $\mathcal{P}^{(n)}$ are orthogonal projection operators onto the subspaces $\mathcal{Q}^{(n)}$ and $\mathcal{P}^{(n)}$, respectively.

The operators fulfill the following relations of orthogonality:

$$\begin{aligned} \mathcal{Q}^{(n)} \mathcal{Q}^{(m)} &= \delta_{nm} \mathcal{Q}^{(n)}, \\ \mathcal{P}^{(n)} \mathcal{P}^{(m)} &= \delta_{nm} \mathcal{P}^{(n)}, \\ \mathcal{Q}^{(n)} \mathcal{P}^{(m)} &= \mathcal{P}^{(n)} \mathcal{Q}^{(m)} = 0. \end{aligned} \quad (9)$$

In the next, one considers the following approximation:

$$1 \approx \sum_{n=0}^1 (\mathcal{Q}^{(n)} + \mathcal{P}^{(n)}). \quad (10)$$

This assumption is a consequence of the fact that we are neglecting all multiphoton cascade transitions. In fact, as one

can see later, even the M1 transitions (magnetic dipole) have negligible contribution to the light-shift.

The projector $Q^{(0)}$ can be written as

$$Q^{(0)} = \sum_d |d\rangle\langle d|, \quad (11)$$

where $|d\rangle$ are the discrete eigenstates of the \mathcal{H}_e Hamiltonian. Further, one may define $Q^{(1)}$ with the help of creation and annihilation operators:

$$Q^{(1)} = \sum_d \sum_{\mathbf{k}\lambda} a_{\mathbf{k}\lambda}^\dagger |d\rangle\langle d| a_{\mathbf{k}\lambda}. \quad (12)$$

In a similar way, one may construct $P^{(0)}$ and $P^{(1)}$ projectors:

$$P^{(0)} = \sum_\alpha \int dE |\alpha E\rangle\langle \alpha E|, \quad (13)$$

$$P^{(1)} = \sum_\alpha \int dE \sum_{\mathbf{k}\lambda} a_{\mathbf{k}\lambda}^\dagger |\alpha E\rangle\langle \alpha E| a_{\mathbf{k}\lambda},$$

where E is the energy of the continuum state, and α stays for other relevant quantum numbers.

C. T -matrix expansion

We try the following ansatz for the light-shift of the state $|i\rangle$:

$$\Delta E_{cs}(i) \equiv A_0 \Re \lim_{\varepsilon \rightarrow 0_+} \langle i | T(E_{op} + i\varepsilon) | i \rangle, \quad (14)$$

where $A_0 = \frac{\mathcal{E}^2 c^2}{\omega_{\mathbf{k}}^2}$, with \mathcal{E} the electric mean-field strength created by the laser and $\omega_{\mathbf{k}}$ the laser frequency. The energy E_{op} is the energy of the one-photon excited-state absorption, i.e., $E_{op} = E_i + \hbar\omega_{\mathbf{k}}$, and cs stands for the cs-like analyzed ion. For H-like ions, the above definition gives the same light-shift formula as the S -matrix expansion [29,30]. The formula (14) is not limited to the H-like ions; it has successfully been used in other many-body problems, for example, in the intershell trielectronic recombination [6], showing very good agreement with the experimental results. Moreover, the T -operator technique has also recently been applied to the scattering-theory analysis of laser-assisted electron impact ionization of He [31].

In this section, we are focusing on the computation of the transition operator T . By definition, one may write [5]

$$T(z) = \mathcal{V} + \mathcal{V} G(z) \mathcal{V}, \quad (15)$$

where

$$G(z) = [z - \mathcal{H}]^{-1} \quad (16)$$

is the Green operator of the total Hamiltonian,

$$\mathcal{V} = \mathcal{H} - \mathcal{H}_0, \quad (17)$$

and z is a complex energy variable. The perturbative expression of $G(z)$ is based on the Lippmann-Schwinger equation

$$G(z) = G_0(z) + G_0(z) \mathcal{V} G(z), \quad (18)$$

with $G_0(z) = [z - \mathcal{H}_0]^{-1}$ being the Green operator of the unperturbed Hamiltonian. An equivalent form of the Lippmann-Schwinger equation is

$$G(z) = G_0(z) + G(z) \mathcal{V} G_0(z). \quad (19)$$

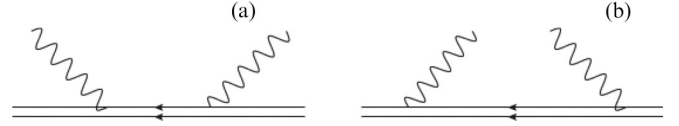


FIG. 2. The diagrams are representing the lowest-order perturbative light-shift correction. The Coulomb-dressed electron is depicted by a double line and the wavy lines represent photons.

Calling the iterative solution of the Lippmann-Schwinger equation together with Eq. (15) gives

$$T^{(n)} = \mathcal{V} + \mathcal{V} G_0 \mathcal{V} + \mathcal{V} G_0 \mathcal{V} G_0 \mathcal{V} + \dots \quad (20)$$

Using Eq. (10), one can write

$$\mathcal{H} \rightarrow 1 \mathcal{H} 1 \equiv \mathcal{H}_0 + \mathcal{V}, \quad (21)$$

where \mathcal{H}_0 is defined as

$$\mathcal{H}_0 = Q^{(0)} \mathcal{H} Q^{(0)} + Q^{(1)} \mathcal{H} Q^{(1)} + P^{(0)} \mathcal{H} P^{(0)} + P^{(1)} \mathcal{H} P^{(1)}, \quad (22)$$

and \mathcal{V} is given by

$$\begin{aligned} \mathcal{V} = & Q^{(0)} \mathcal{H} Q^{(1)} + Q^{(0)} \mathcal{H} P^{(0)} + Q^{(0)} \mathcal{H} P^{(1)} \\ & + Q^{(1)} \mathcal{H} Q^{(0)} + Q^{(1)} \mathcal{H} P^{(0)} + Q^{(1)} \mathcal{H} P^{(1)} \\ & + P^{(0)} \mathcal{H} Q^{(0)} + P^{(0)} \mathcal{H} Q^{(1)} + P^{(0)} \mathcal{H} P^{(1)} \\ & + P^{(1)} \mathcal{H} Q^{(0)} + P^{(1)} \mathcal{H} Q^{(1)} + P^{(1)} \mathcal{H} P^{(0)}. \end{aligned} \quad (23)$$

In the process of laser-ion interaction, one expects to see a photoexcitation followed almost simultaneously by a photodeexcitation. However, one may have a counterintuitive process: first a photodeexcitation and then a photoexcitation as was depicted in Fig. 2. In the second-order of perturbation theory, the projection of the transition matrix (20) on the relevant subspace $Q^{(1)}$ gives

$$\begin{aligned} Q^{(1)} T Q^{(1)} \approx & Q^{(1)} \mathcal{V} Q^{(0)} G_0 Q^{(0)} \mathcal{V} Q^{(1)} \\ & + Q^{(1)} \mathcal{V} P^{(0)} G_0 P^{(0)} \mathcal{V} Q^{(1)}, \end{aligned} \quad (24)$$

or more precisely,

$$\begin{aligned} Q^{(1)} T Q^{(1)} \approx & Q^{(1)} \mathcal{H}_{er} Q^{(0)} G_0 Q^{(0)} \mathcal{H}_{er} Q^{(1)} \\ & + Q^{(1)} \mathcal{H}_{er} P^{(0)} G_0 P^{(0)} \mathcal{H}_{er} Q^{(1)}. \end{aligned} \quad (25)$$

One should mention that in Eqs. (24) and (25) we have kept just the conservative terms. Further, in the third order of perturbation theory we have

$$\begin{aligned} Q^{(1)} T Q^{(1)} \approx & Q^{(1)} \mathcal{V} G_0 \mathcal{V} G_0 \mathcal{V} Q^{(1)} \\ \approx & Q^{(1)} \mathcal{V} Q^{(0)} G_0 Q^{(0)} \mathcal{V} Q^{(0)} G_0 Q^{(0)} \mathcal{V} Q^{(1)} \\ & + Q^{(1)} \mathcal{V} P^{(0)} G_0 P^{(0)} \mathcal{V} P^{(0)} G_0 P^{(0)} \mathcal{V} Q^{(1)} \\ = & 0, \end{aligned} \quad (26)$$

because $Q^{(0)} \mathcal{V} Q^{(0)} = 0$ and $P^{(0)} \mathcal{V} P^{(0)} = 0$.

In the fourth order of perturbation theory, one can write

$$\begin{aligned} Q^{(1)} T Q^{(1)} \approx & Q^{(1)} \mathcal{H}_{er} Q^{(0)} G_0 Q^{(0)} \mathcal{H}_e P^{(0)} G_0 \\ & \times P^{(0)} \mathcal{H}_e Q^{(0)} G_0 Q^{(0)} \mathcal{H}_{er} Q^{(1)} \quad (a) \\ & + Q^{(1)} \mathcal{H}_{er} Q^{(0)} G_0 Q^{(0)} \mathcal{H}_{er} Q^{(1)} G_0 \\ & \times Q^{(1)} \mathcal{H}_{er} Q^{(0)} G_0 Q^{(0)} \mathcal{H}_{er} Q^{(1)} \quad (b) \end{aligned}$$

$$\begin{aligned}
& + Q^{(1)} \mathcal{H}_{er} Q^{(0)} G_0 Q^{(0)} \mathcal{H}_{er} P^{(1)} G_0 \\
& \times P^{(1)} \mathcal{H}_{er} Q^{(0)} G_0 Q^{(0)} \mathcal{H}_{er} Q^{(1)} \quad (c) \\
& + Q^{(1)} \mathcal{H}_{er} P^{(0)} G_0 P^{(0)} \mathcal{H}_e Q^{(0)} G_0 \\
& \times Q^{(0)} \mathcal{H}_e P^{(0)} G_0 P^{(0)} \mathcal{H}_{er} Q^{(1)} \quad (d) \\
& + Q^{(1)} \mathcal{H}_{er} P^{(0)} G_0 P^{(0)} \mathcal{H}_{er} Q^{(1)} G_0 \\
& \times Q^{(1)} \mathcal{H}_{er} P^{(0)} G_0 P^{(0)} \mathcal{H}_{er} Q^{(1)} \quad (e) \\
& + Q^{(1)} \mathcal{H}_{er} P^{(0)} G_0 P^{(0)} \mathcal{H}_{er} P^{(1)} G_0 \\
& \times P^{(1)} \mathcal{H}_{er} P^{(0)} G_0 P^{(0)} \mathcal{H}_{er} Q^{(1)}. \quad (f) \quad (27)
\end{aligned}$$

It is worth mentioning that all components of Eq. (27) correspond to virtual physical processes, represented and named in Fig. 4.

In order to compute the transition matrix element in Eq. (14), one should define both states involved in the process (see Fig. 1): the the initial state, identical to the final one, is made up by a bound state and a photon, i.e., $|i\rangle = |q\rangle \otimes |1; \mathbf{k}\lambda\rangle$, and the intermediate state is a bound $|q\rangle$ or a continuum $|\alpha E\rangle$ state; and the notation $|1; \mathbf{k}\lambda\rangle$ stands for a uniphotonic state. It is easy to check that

$$Q^{(1)}|i\rangle = |i\rangle. \quad (28)$$

It is not difficult to compute the following useful relations:

$$\begin{aligned}
Q^{(0)} G_0(z) Q^{(0)} &= \sum_q \frac{|q\rangle \langle q|}{z - E_q}, \\
Q^{(1)} G_0(z) Q^{(1)} &= \sum_{\lambda q} \int k^2 dk d\Omega_{\mathbf{k}} \frac{a_{\mathbf{k}\lambda}^\dagger |q\rangle \langle q| a_{\mathbf{k}\lambda}}{z - E_q - \hbar\omega_{\mathbf{k}}}, \\
P^{(0)} G_0(z) P^{(0)} &= \sum_\alpha \int dE \frac{|\alpha E\rangle \langle \alpha E|}{z - E}, \\
P^{(1)} G_0(z) P^{(1)} &= \sum_{\lambda\alpha} \int k^2 dk d\Omega_{\mathbf{k}} dE \frac{a_{\mathbf{k}\lambda}^\dagger |\alpha E\rangle \langle \alpha E| a_{\mathbf{k}\lambda}}{z - E - \hbar\omega_{\mathbf{k}}},
\end{aligned} \quad (29)$$

and inserting them into Eq. (25), we find out that the light-shift is proportional to

$$\sum_q \frac{\langle i | \mathcal{H}_{er} | q \rangle \langle q | \mathcal{H}_{er} | i \rangle}{z - E_q}, \quad (30)$$

with the mention that for continuous intermediate states the sum changes into an integral. This second-order contribution was represented in Fig. 2(a). Further, in the fourth order of perturbation theory (see Fig. 3), from Eq. (27) (a) one may see that the light-shift is proportional to

$$\sum_q \frac{|\langle i | \mathcal{H}_{er} | q \rangle|^2}{(z - E_q)^2} \sum_\alpha \int dE \frac{|\langle q | \mathcal{H}_e | \alpha E \rangle|^2}{z - E}, \quad (31)$$

and from Eq. (27) (b) and Eq. (27) (c) one should have two other contributions:

$$\sum_q \frac{|\langle i | \mathcal{H}_{er} | q \rangle|^2}{(z - E_q)^2} \sum_\lambda \int k^2 dk d\Omega_{\mathbf{k}} \frac{|\langle q | \mathcal{H}_{er} a_{\mathbf{k}\lambda}^\dagger | q \rangle|^2}{z - E_q - \hbar\omega_{\mathbf{k}}} \quad (32)$$

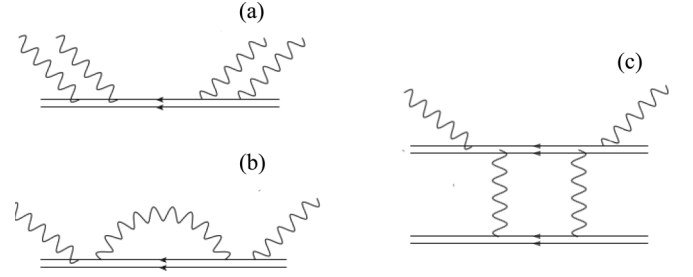


FIG. 3. The diagrams are representing the fourth-order perturbative light-shift correction, where the Coulomb-dressed electron is depicted by a double line and the wavy lines represent photons: (a) electron excitation, (b) self-energy correction, and (c) electron correction via Coulomb field.

and

$$\sum_q \frac{|\langle i | \mathcal{H}_{er} | q \rangle|^2}{(z - E_q)^2} \sum_\lambda \int k^2 dk d\Omega_{\mathbf{k}} \frac{|\langle q | \mathcal{H}_{er} a_{\mathbf{k}\lambda}^\dagger | \alpha E \rangle|^2}{z - E - \hbar\omega_{\mathbf{k}}}, \quad (33)$$

respectively; for continuous states, the sum transforms into an integral. Using the same procedure, one may write the terms (27) (d), (e), and (f) in a more suitable form, i.e.,

$$\sum_\alpha \int dE \frac{|\langle i | \mathcal{H}_{er} | \alpha E \rangle|^2}{(z - E)^2} \sum_q \frac{|\langle \alpha E | \mathcal{H}_e | q \rangle|^2}{z - E_q}, \quad (34)$$

$$\begin{aligned}
& \sum_\alpha \int dE \frac{|\langle i | \mathcal{H}_{er} | \alpha E \rangle|^2}{(z - E)^2} \\
& \times \sum_{\lambda q} \int k^2 dk d\Omega_{\mathbf{k}} \frac{|\langle \alpha E | \mathcal{H}_{er} a_{\mathbf{k}\lambda}^\dagger | q \rangle|^2}{z - E_q - \hbar\omega_{\mathbf{k}}}, \quad (35)
\end{aligned}$$

and

$$\begin{aligned}
& \sum_\alpha \int dE \frac{|\langle i | \mathcal{H}_{er} | \alpha E \rangle|^2}{(z - E)^2} \\
& \times \sum_{\lambda\alpha} \int k^2 dk d\Omega_{\mathbf{k}} dE \frac{|\langle \alpha E | \mathcal{H}_{er} a_{\mathbf{k}\lambda}^\dagger | \alpha E \rangle|^2}{z - E - \hbar\omega_{\mathbf{k}}}. \quad (36)
\end{aligned}$$

At this point, we have all the contributions we need in our theory. In order to get the above expressions, we have used an approximation called isolated resonances (whereby one neglects the off-diagonal matrix elements of the propagators).

In order to compute the light-shift energy levels, in the main formula (14) one should take the limit $\varepsilon \rightarrow 0_+$. Using the formula [4]

$$\lim_{\varepsilon \rightarrow 0_+} \frac{1}{x + i\varepsilon} = \text{P}\left(\frac{1}{x}\right) - i\pi\delta(x), \quad (37)$$

where P is the principal part, one may transform the Eqs. (31) and (34) into

$$\lim_{\varepsilon \rightarrow 0_+} \sum_\alpha \int dE \frac{|\langle q | \mathcal{H}_e | \alpha E \rangle|^2}{z - E} = \Delta E_q^C - i\Gamma_q^C/2, \quad (38)$$

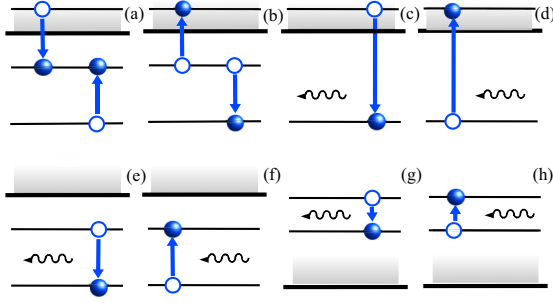


FIG. 4. In this figure we are scatching some elementary processes, those module square are giving sens to the diagrams represented in Fig 3; (a) dielectronic recombination via Coulomb interaction $Q^{(0)}\mathcal{H}_e P^{(0)}$, (b) Auger process via Coulomb interaction $P^{(0)}\mathcal{H}_e Q^{(0)}$, (c) radiative recombination $Q^{(1)}\mathcal{H}_e P^{(0)}$, (d) photoeffect $P^{(0)}\mathcal{H}_e Q^{(1)}$, (e) photon de-excitation $Q^{(1)}\mathcal{H}_e Q^{(0)}$, (f) photon absorption (excitation) $Q^{(0)}\mathcal{H}_e Q^{(1)}$, (g) Bremsstrahlung $P^{(1)}\mathcal{H}_e P^{(0)}$, and (h) excitation (inverse of Bremsstrahlung) $P^{(0)}\mathcal{H}_e P^{(1)}$.

where the Coulomb energy correction ΔE_q^C and the Auger width Γ_q^C have the expressions

$$\Delta E_q^C \equiv P \sum_{\alpha} \int dE \frac{|\langle q | \mathcal{H}_e | \alpha E \rangle|^2}{z - E}, \quad (39)$$

$$\Gamma_q^C \equiv 2\pi \sum_{\alpha} |\langle q | \mathcal{H}_e | \alpha E_q \rangle|^2,$$

and where we have used in the second equation $z = E$. Furthermore, if one makes the definitions

$$\Delta E_q^R = P \sum_{\lambda} \int k^2 dk d\Omega_{\mathbf{k}} \sum_q \frac{|\langle q | \mathcal{H}_e a_{\mathbf{k}\lambda}^{\dagger} | q \rangle|^2}{z - E_q - \hbar\omega_{\mathbf{k}}}, \quad (40)$$

$$\Gamma_q^R = 2\pi \sum_{\lambda} \int k^2 dk d\Omega_{\mathbf{k}} |\langle q | \mathcal{H}_e a_{\mathbf{k}\lambda}^{\dagger} | q \rangle|^2,$$

with $z = E_q + \hbar\omega_{\mathbf{k}}$, one find that the middle part of the expressions (32), (33), (35), and (36) is

$$\lim_{\varepsilon \rightarrow 0^+} \sum_{\lambda} \int k^2 dk d\Omega_{\mathbf{k}} \sum_q \frac{|\langle q | \mathcal{H}_e a_{\mathbf{k}\lambda}^{\dagger} | q \rangle|^2}{z - E_q - \hbar\omega_{\mathbf{k}}} = \Delta E_q^R - i\Gamma_q^R/2. \quad (41)$$

In the above expressions, we have denoted by ΔE_q^R the self-energy and one-photon exchange corrections for the intermediate state $|q\rangle$, and by Γ_q^R the radiative width of the state.

In Fig. 4 we are describing the elementary processes corresponding to transitions described by the different nondiagonal matrix elements. The fourth-order processes in Eq. (27) are shown by the diagrams in Fig. 3. The Feynman diagrams for virtual two-photon exchange between bound electrons involving two different time orderings are known as the ‘‘ladder’’ and the ‘‘crossed-photon’’ diagrams [16]. It is easy to put the expressions (34)–(36) into the form of the definitions (40) and (41) by replacing the bound states with the continuous ones.

As we have seen, using the quantum mechanics formalism one may describe the situations (a), (b), and (c), represented in Fig. 3. In order to complete our theory, one should introduce by hand the radiative corrections, i.e., screened Lamb shift

diagrams, which are purely QED processes; anyhow, it has just a real part, and consequently has contributions only to the energies. So, in the fourth order of perturbation theory, one may write the level-shift expression as

$$\Delta E_{cs}(i) = A_0 \sum_q \langle i | \mathcal{H}_{er} | q \rangle \left(1 + \frac{\Delta E_q - i\Gamma_q/2}{z - E_q} \right) \times \frac{\langle q | \mathcal{H}_{er} | i \rangle}{z - E_q}, \quad (42)$$

where we made the notations $\Delta E_q = \Delta E_q^C + \Delta E_q^R + \Delta E_q^{VP}$ and $\Gamma_q = \Gamma_q^C + \Gamma_q^R$, and where ΔE_q^{VP} represents the vacuum polarization correction to the energies. It is not difficult to see that, in higher order of perturbation theory, one gets the following contributions:

$$1 + \frac{\Delta E_q - i\Gamma_q/2}{z - E_q} + \left(\frac{\Delta E_q - i\Gamma_q/2}{z - E_q} \right)^2 \dots, \quad (43)$$

and using the formula [8]

$$\sum_{n=0}^{\infty} x^n = \frac{1}{1-x} \quad \text{if } |x| < 1, \quad (44)$$

we get from (14) the expression

$$\Delta E_{cs}(i) = A_0 \sum_q \frac{\langle i | \mathcal{H}_{er} | q \rangle \langle q | \mathcal{H}_{er} | i \rangle}{E_i + \hbar\omega_{\mathbf{k}} - E_q - \Delta E_q - i\Gamma_q/2}. \quad (45)$$

It should be noted that arriving to the formula (43), the resonance approximation is made again.

The formula (14) describes the so-called rotating-wave approximation, a situation represented in Fig. 2(a). In order to include in our computations the counterintuitive process represented in Fig. 2(b), the parameter E_{op} in Eq. (14) should be redefined to $E_{op} = E_i - \hbar\omega_{\mathbf{k}}$. Applying a similar treatment to Fig. 2(b), one gets

$$\Delta E'_{cs}(i) = A_0 \sum_q \frac{\langle i | \mathcal{H}_{er} | q \rangle \langle q | \mathcal{H}_{er} | i \rangle}{E_i - \hbar\omega_{\mathbf{k}} - E_q - \Delta E_q - i\Gamma_q/2}, \quad (46)$$

and finally, we are able to write down the total light-shift, which is the sum of the above two expressions (45) and (46).

The dynamic level-shift energy levels in a classical framework with an adiabatically damped laser-atom interaction and a treatment based on time-independent perturbation theory, with a second-quantized laser-atom dipole interaction Hamiltonian, are equivalent [30]. Therefore, our further calculations are based on the semiclassical approach.

D. The theory of He-like light-shift

The hydrogenlike relativistic light-shift of a given atomic state $i' \equiv |n_i \kappa_i\rangle$ is given by [14]

$$\Delta E_H(i') = A_0 \sum_{n_v \kappa_v} \left(\frac{\langle n_i \kappa_i | V_2^{JM} | n_v \kappa_v \rangle \langle n_v \kappa_v | V_1^{JM} | n_i \kappa_i \rangle}{E_i - E_v - \hbar\omega_{\mathbf{k}}} + \frac{\langle n_i \kappa_i | V_1^{JM} | n_v \kappa_v \rangle \langle n_v \kappa_v | V_2^{JM} | n_i \kappa_i \rangle}{E_i - E_v + \hbar\omega_{\mathbf{k}}} \right), \quad (47)$$

with $V_1^{JM} = -\boldsymbol{\alpha} \cdot \hat{\boldsymbol{\epsilon}}_v e^{i\mathbf{k}\cdot\mathbf{r}}$ and $V_2^{JM} = -\boldsymbol{\alpha}^* \cdot \hat{\boldsymbol{\epsilon}}_v^* e^{-i\mathbf{k}\cdot\mathbf{r}}$. A_0 is given by $A_0 = \frac{\mathcal{E}^2 c^2}{\omega_{\mathbf{k}}^2}$, with \mathcal{E} being the electric field strength, $|n_i \kappa_i\rangle$ and $|n_v \kappa_v\rangle$ are eigenfunctions of the unperturbed

Hamiltonian \mathcal{H}_0 with the corresponding energies E_i and E_v , respectively, and $\omega_{\mathbf{k}}$ is the laser frequency. Note that the sum over the intermediate states is a generalized sum, as continuum states are included into it. The quantum numbers J and M appear due to the spherical expansion of the exponential [23]

$$e^{i\mathbf{k}\cdot\mathbf{r}} = 4\pi \sum_{JM} i^J j_J(kr) Y_{JM}^*(\hat{k}) Y_{JM}(\hat{r}), \quad (48)$$

where $j_J(kr)$ is the spherical Bessel function [32]. The vector $\mathbf{k} \equiv k\hat{k}$ is called the propagation vector, and we consider the electromagnetic plane waves always propagating in the \hat{k} direction.

In order to describe He-like systems, we introduce some useful notations: in the independent particle model, the initial state, identical with the final one, is $i \equiv |(n_i\kappa_i, n_0\kappa_0) J_i M_i\rangle$, while the intermediate (virtual) states are denoted by $|v \equiv |(n_v\kappa_v, n_0\kappa_0) J_v M_v\rangle$. With this notation, Eqs. (45) and (46) become

$$\begin{aligned} \Delta E_{\text{He}(i)} &= A_0 \sum_{n_v\kappa_v J_v M_v} \left(\frac{\langle (n_0\kappa_0, n_i\kappa_i) J_i M_i | V_2^{JM} | (n_0\kappa_0, n_v\kappa_v) J_v M_v \rangle}{E_i - E_v - \hbar\omega_{\mathbf{k}}} \right. \\ &\quad \times \langle (n_0\kappa_0, n_v\kappa_v) J_v M_v | V_1^{JM} | (n_0\kappa_0, n_i\kappa_i) J_i M_i \rangle \\ &\quad + \frac{\langle (n_0\kappa_0, n_i\kappa_i) J_i M_i | V_1^{JM} | (n_0\kappa_0, n_v\kappa_v) J_v M_v \rangle}{E_i - E_v + \hbar\omega_{\mathbf{k}}} \\ &\quad \left. \times \langle (n_0\kappa_0, n_v\kappa_v) J_v M_v | V_2^{JM} | (n_0\kappa_0, n_i\kappa_i) J_i M_i \rangle \right). \quad (49) \end{aligned}$$

The contribution of the Lamb shift [22] to the light-shift denominator of Eq. (47) for two-photon $1s - 2s$ transition is 0.02% in Fe and 0.2% in U. As we discuss later, even the magnetic one-photon transitions give a bigger contribution. In this paper, we are focusing on the light-shift of two-photon transitions, and the decay widths are important only at resonances (when the detuning is comparable to or less than the decay width). The decay widths [23] of the $2s$ state ($\approx 2 \times 10^{-7}$ eV in Fe and ≈ 0.1 eV in U) give even smaller contribution to the light-shift in the $1s - 2s$ transition than the Lamb shift of the $1s$ state. Consequently, in our formula we are neglecting both Lamb and decay width inputs, which are important only at resonances.

E. Decomposition into H-like matrix elements

Assuming that we know how to compute Eq. (47), our task is to express the He-like light-shift (49) in terms of the H-like light-shift. In order to do this, we are expressing all matrix elements of the type

$$\langle (n_0\kappa_0, n_i\kappa_i) J_i M_i | V_2^{JM} | (n_0\kappa_0, n_v\kappa_v) J_v M_v \rangle, \quad (50)$$

as functions of H-like matrix elements.

In the IPM model, the many-fermionic wave function $|i \equiv |(n_0\kappa_0, n_i\kappa_i) J_i M_i\rangle$ is given by the Slater determinant,

$$\begin{aligned} |(n_0\kappa_0, n_i\kappa_i) J_i M_i \rangle &= \frac{1}{N} \sum_{m_0 m_i} C(j_0 j_i J_i; m_0 m_i M_i) \\ &\quad \times \begin{vmatrix} |n_0\kappa_0 m_0 \rangle & |n_i\kappa_i m_i \rangle \\ |n_0\kappa_0 m_0 \rangle & |n_i\kappa_i m_i \rangle \end{vmatrix}, \quad (51) \end{aligned}$$

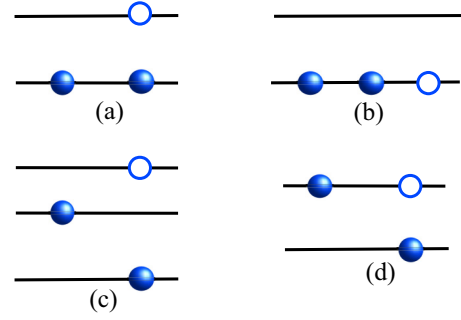


FIG. 5. The diagrams of all possible configurations in He-like systems: (a) $|n_i\kappa_i\rangle = |n_0\kappa_0\rangle$, $|n_v\kappa_v\rangle \neq |n_i\kappa_i\rangle$, and $|n_v\kappa_v\rangle \neq |n_0\kappa_0\rangle$; (b) $|n_i\kappa_i\rangle = |n_0\kappa_0\rangle$, $|n_v\kappa_v\rangle = |n_i\kappa_i\rangle$, and $|n_v\kappa_v\rangle = |n_0\kappa_0\rangle$; (c) $|n_i\kappa_i\rangle \neq |n_0\kappa_0\rangle$, $|n_v\kappa_v\rangle \neq |n_i\kappa_i\rangle$, and $|n_v\kappa_v\rangle \neq |n_0\kappa_0\rangle$; (d) $|n_i\kappa_i\rangle \neq |n_0\kappa_0\rangle$, $|n_v\kappa_v\rangle \neq |n_i\kappa_i\rangle$, and $|n_v\kappa_v\rangle = |n_0\kappa_0\rangle$.

where $N = \sqrt{2}$ if $|n_0\kappa_0\rangle \neq |n_i\kappa_i\rangle$ and $N = 2$ if $|n_0\kappa_0\rangle = |n_i\kappa_i\rangle$. The coefficient $C(j_1 j_2 J; m_1 m_2 M)$ is called the Clebsch-Gordan coefficient [33]; for a given j_1 and j_2 the values of J are restricted by the triangular condition $j_1 + j_2 \geq J \geq |j_1 - j_2|$, and J ranges from $j_1 + j_2$ down to $|j_1 - j_2|$ in integer steps. The coefficient vanishes unless $M = m_1 + m_2$.

In the He-like ions, one may have only two distinct configurations: (1) in which both electrons are on the same subshell, the situation presented in Figs. 5(a) and 5(b), and (2) where the two electrons are on different subshells, the situation presented in Figs. 5(c) and 5(d).

(1) Let us consider first the case drawn in Fig. 5(a), i.e., $|n_i\kappa_i\rangle = |n_0\kappa_0\rangle$, $|n_v\kappa_v\rangle \neq |n_i\kappa_i\rangle$, and $|n_v\kappa_v\rangle \neq |n_0\kappa_0\rangle$. The expression of the initial wave function $|i \equiv |(n_0\kappa_0, n_i\kappa_i) J_i M_i\rangle$ is given by Eq. (51) with $N = 2$, and the expression of the intermediate wave function $|v \equiv |(n_0\kappa_0, n_v\kappa_v) J_v M_v\rangle$ is given by

$$\begin{aligned} |(n_0\kappa_0, n_v\kappa_v) J_v M_v \rangle &= \frac{1}{\sqrt{2}} \sum_{m'_0 m'_v} C(j_0 j_v J_v; m'_0 m'_v M_v) \\ &\quad \times \begin{vmatrix} |n_0\kappa_0 m'_0 \rangle & |n_v\kappa_v m'_v \rangle \\ |n_0\kappa_0 m'_0 \rangle & |n_v\kappa_v m'_v \rangle \end{vmatrix}. \quad (52) \end{aligned}$$

Farther, by using Eqs. (51) and (52) one may compute the matrix element (50); it is not difficult to find that

$$\begin{aligned} \langle (n_0\kappa_0, n_i\kappa_i) J_i M_i | V_2^{JM} | (n_0\kappa_0, n_v\kappa_v) J_v M_v \rangle &= \frac{1}{\sqrt{2}} \sum_{m_0 m_i m'_0 m'_v} C(j_0 j_i J_i; m_0 m_i M_i) \\ &\quad \times C(j_0 j_v J_v; m'_0 m'_v M_v) (\delta_{m_0 m'_0} \langle n_i\kappa_i m_i | V_2^{JM} | n_v\kappa_v m'_v \rangle \\ &\quad - \delta_{m_i m'_0} \langle n_0\kappa_0 m_0 | V_2^{JM} | n_v\kappa_v m'_v \rangle). \quad (53) \end{aligned}$$

In this result, we have used the orthogonality property of the wave functions, i.e., $\langle n_i\kappa_i m_i | n_v\kappa_v m'_v \rangle = 0$, $\langle n_0\kappa_0 m_0 | n_v\kappa_v m'_v \rangle = 0$ and $\langle n_0\kappa_0 m_0 | n_0\kappa_0 m'_0 \rangle = \delta_{m_0 m'_0}$.

To simplify Eq. (53), one should use the Wigner-Eckart theorem [33]

$$\begin{aligned} \langle \alpha_a j_a m_a | T^{JM} | \alpha_b j_b m_b \rangle &= \frac{1}{\sqrt{2j_a + 1}} C(j_b J j_a; m_b M m_a) \langle \alpha_a j_a || T^J || \alpha_b j_b \rangle, \quad (54) \end{aligned}$$

where T^{JM} is a tensor operator of rank J , and α stands for any other quantum number (for example, the parity). The reduced matrix element $\langle \alpha_a j_a || T_L || \alpha_b j_b \rangle$ is independent of M , m_a , and m_b .

In order to perform the summation over all magnetic quantum numbers, one should use the relation [33]

$$\sum_{\alpha\beta\delta} C(abc; \alpha\beta\gamma) C(afd; \alpha\xi\delta) C(dbe; \delta\beta\epsilon) = (-1)^{b+c+d+f} \sqrt{1+2c} \sqrt{1+2d} \begin{Bmatrix} a & b & c \\ e & f & d \end{Bmatrix} C(cfe; \gamma\xi\epsilon), \quad (55)$$

where $\{...\}$ is a 6- j symbol.

After long but straightforward computations, one obtains the final expression of Eq. (53):

$$\begin{aligned} & \langle (n_0\kappa_0, n_i\kappa_i) J_i M_i | V_2^{JM} | (n_0\kappa_0, n_v\kappa_v) J_v M_v \rangle \\ &= \frac{1}{\sqrt{2}} (-1)^{3j_i+j_v+J} [(-1)^{2j_i+J_i} - 1] \sqrt{2J_v+1} \langle n_i\kappa_i || V_2^J || n_v\kappa_v \rangle \begin{Bmatrix} j_v & j_i & J_v \\ J_i & J & j_i \end{Bmatrix} C(J_v J J_i; M_v M M_i). \end{aligned} \quad (56)$$

To get Eq. (56), we have to use the Clebsch-Gordan coefficients property [33]

$$C(abc; \alpha\beta\gamma) = (-1)^{a+b-c} C(bac; \beta\alpha\gamma). \quad (57)$$

To compute the matrix element (49), one should apply the same method. The result is given by

$$\begin{aligned} & \langle (n_0\kappa_0, n_v\kappa_v) J_v M_v | V_1^{JM} | (n_0\kappa_0, n_i\kappa_i) J_i M_i \rangle \\ &= \frac{1}{\sqrt{2}} (-1)^{2j_i+2j_v-J_v+J_i+J} [(-1)^{2j_i-J_i} - 1] \sqrt{2J_i+1} \langle n_v\kappa_v || V_1^J || n_i\kappa_i \rangle \begin{Bmatrix} j_i & j_i & J_i \\ J_v & J & j_v \end{Bmatrix} C(J_i J J_v; M_i M M_v). \end{aligned} \quad (58)$$

It is enough to introduce Eqs. (56) and (58) into Eq. (49) in order to get

$$\begin{aligned} \Delta E_{\text{He}}(i) = & -A_0 \sum_{n_v \neq n_i, \kappa_v, J_v, M_v} (-1)^{5j_i+3j_v-J_v+J_i+2J} [(-1)^{2j_i-J_i} - 1] \sqrt{2J_v+1} \sqrt{2J_i+1} \begin{Bmatrix} j_v & j_i & J_v \\ J_i & J & j_i \end{Bmatrix} \begin{Bmatrix} j_i & j_i & J_i \\ J_v & J & j_v \end{Bmatrix} \\ & \times C(J_v J J_i; M_v M M_i) C(J_i J J_v; M_i M M_v) \left(\frac{\langle n_i\kappa_i || V_2^J || n_v\kappa_v \rangle \langle n_v\kappa_v || V_1^J || n_i\kappa_i \rangle}{E_i - E_v - \hbar\omega_{\mathbf{k}}} + \frac{\langle n_i\kappa_i || V_1^J || n_v\kappa_v \rangle \langle n_v\kappa_v || V_2^J || n_i\kappa_i \rangle}{E_i - E_v + \hbar\omega_{\mathbf{k}}} \right). \end{aligned} \quad (59)$$

Now let us consider the situation of Fig. 5(b), i.e., $|n_i\kappa_i\rangle = |n_0\kappa_0\rangle = |n_v\kappa_v\rangle$. Following the same method as in the previous case, we are able to put the light-shift in the form

$$\begin{aligned} \Delta E_{\text{He}}(i) = & \frac{1}{4} A_0 \Re \left\{ \sum_{J_v, M_v} (-1)^{J_i+J_v} \sqrt{2J_v+1} \sqrt{2J_i+1} [(-1)^{J_i} + 1] [(-1)^{J_v} + 1] \begin{Bmatrix} j_i & j_i & J_i \\ J_v & J & j_i \end{Bmatrix} \begin{Bmatrix} j_i & j_i & J_i \\ J_i & J & j_i \end{Bmatrix} \right. \\ & \times C(J_v J J_i; M_v M M_i) C(J_i J J_v; M_i M M_v) \left. \left(\frac{\langle n_i\kappa_i || V_2^J || n_i\kappa_i \rangle \langle n_i\kappa_i || V_1^J || n_i\kappa_i \rangle}{E_i - E_i - \hbar\omega_{\mathbf{k}} - i\Gamma_i/2} + \frac{\langle n_i\kappa_i || V_1^J || n_i\kappa_i \rangle \langle n_i\kappa_i || V_2^J || n_i\kappa_i \rangle}{E_i - E_i + \hbar\omega_{\mathbf{k}} - i\Gamma_i/2} \right) \right\}. \end{aligned} \quad (60)$$

Due to the expression in the last parenthesis, this contribution is always zero; the reduced matrix elements are real, and the contribution is

$$\Re \left[\frac{1}{-\hbar\omega_{\mathbf{k}} - i\Gamma_i/2} + \frac{1}{\hbar\omega_{\mathbf{k}} - i\Gamma_i/2} \right] = 0. \quad (61)$$

In conclusion, in case we have both electrons in the same subshell, the light-shift is given by Eq. (59).

(2) For the situation depicted in Fig. 5(c), i.e., $|n_i\kappa_i\rangle \neq |n_0\kappa_0\rangle$, $|n_v\kappa_v\rangle \neq |n_i\kappa_i\rangle$, and $|n_v\kappa_v\rangle \neq |n_0\kappa_0\rangle$, the light-shift is

$$\begin{aligned} \Delta E_{\text{He}}(i) = & A_0 \sum_{n_v, \kappa_v, J_v, M_v} (-1)^{6j_0+3j_i+3j_v-J_i-J_v+2J} \sqrt{2J_v+1} \sqrt{2J_i+1} \begin{Bmatrix} j_v & j_0 & J_v \\ J_i & J & j_i \end{Bmatrix} \begin{Bmatrix} j_i & j_0 & J_i \\ J_v & J & j_v \end{Bmatrix} C(J_v J J_i; M_v M M_i) \\ & \times C(J_i J J_v; M_i M M_v) \left(\frac{\langle n_i\kappa_i || V_2^J || n_v\kappa_v \rangle \langle n_v\kappa_v || V_1^J || n_i\kappa_i \rangle}{E_i - E_v - \hbar\omega_{\mathbf{k}}} + \frac{\langle n_i\kappa_i || V_1^J || n_v\kappa_v \rangle \langle n_v\kappa_v || V_2^J || n_i\kappa_i \rangle}{E_i - E_v + \hbar\omega_{\mathbf{k}}} \right), \end{aligned} \quad (62)$$

and for the case illustrated in Fig. 5(d), i.e., $|n_i\kappa_i\rangle \neq |n_0\kappa_0\rangle$, $|n_v\kappa_v\rangle \neq |n_i\kappa_i\rangle$, and $|n_v\kappa_v\rangle = |n_0\kappa_0\rangle$, is

$$\begin{aligned} \Delta E_{\text{He}}(i) = & -A_0 \sum_{J_v, M_v} (-1)^{7j_0+3j_i-J_i+2J} (1 + (-1)^{J_v}) \sqrt{2J_v+1} \sqrt{2J_i+1} \begin{Bmatrix} j_i & j_0 & J_i \\ J_v & J & j_0 \end{Bmatrix} \begin{Bmatrix} j_0 & j_0 & J_v \\ J_i & J & j_i \end{Bmatrix} C(J_v J J_i; M_v M M_i) \\ & \times C(J_i J J_v; M_i M M_v) \left(\frac{\langle n_i\kappa_i || V_2^J || n_0\kappa_0 \rangle \langle n_0\kappa_0 || V_1^J || n_i\kappa_i \rangle}{E_i - E_0 - \hbar\omega_{\mathbf{k}}} + \frac{\langle n_i\kappa_i || V_1^J || n_0\kappa_0 \rangle \langle n_0\kappa_0 || V_2^J || n_i\kappa_i \rangle}{E_i - E_0 + \hbar\omega_{\mathbf{k}}} \right). \end{aligned} \quad (63)$$

We conclude that in case we have the two electrons in different subshells, the light-shift is given by the sum of Eqs. (62) and (63).

III. RESULTS

In Eqs. (47) and (49), the generalized series over intermediate states include the bound states, the positive-energy-continuum eigenstates, and also the negative-energy-continuum eigenstates. In order to evaluate these second-order expressions, we have used the Green's function in the Sturmian representation [34]. In this representation, the continuous sum over wave functions will be replaced by discrete summations running over all, positive and negative, integers. It is possible to transform these expressions into forms containing only summations over non-negative integers [34]. In all our numerical results, the number of terms included in the expansion in order to achieve convergence to the number of figures quoted (five places after the decimal point) varied from 5 for $Z = 26$ to 10 for $Z = 91$.

We are starting our discussion on relativistic He-like light-shifts with the $1s^2$ ground state. As one may see in formula (59), the light-shift is proportional to a product of two 6- j symbols. For $J = 1$, the only nonzero results are for $J_v = 1$ and $j_v = \frac{1}{2}$ or $\frac{3}{2}$. The products of the two Clebsch-Gordan coefficients are nonzero only in the special case $M = 0$, which implies $M_i = M_v = 0$. Further, the only unknown quantities in the Eq. (59) are the reduced matrix elements. We want to relate these quantities to the H-like light-shift expression (47), and for this reason one should use the Wigner-Eckart theorem (54). After some elementary computations, one may see that the He-like light-shift is 2 times the H-like light-shift (47), with the extra condition that $n_v \geq 2$. Furthermore, the contribution $n_v = 1$ is zero, for the same reason as we have already discussed in Eq. (61). We conclude that the light-shift of the $1s^2$ ground state is $2 \Delta E_H(1s)$.

For a laser beam pointing in an arbitrary direction \hat{e}_z , one may define the left- and right-handed circular polarizations [23]

$$\epsilon_{\mp} = \frac{1}{\sqrt{2}}(\hat{e}_x \mp i\hat{e}_y). \quad (64)$$

From Eq. (47), one could see that both polarizations give the same result; hence the light-shift does not depend on the laser's polarization.

The independent particle model, where the electron-electron interaction is neglected, works well for highly charged ions. In Fig. 6 we have represented the difference between relativistic and nonrelativistic light-shifts in He-like Fe, for a laser field intensity of $I = 10^{18}$ W/cm². The two plots have different behavior: in the energy interval 6300–6500 eV, ω_{2p} (Bohr formula) is a resonant frequency for the nonrelativistic light-shift, and at the same time $\omega_{2p_{1/2}}$ and $\omega_{2p_{3/2}}$ (Sommerfeld formula) are resonant frequencies for the relativistic light-shift. This behavior gives different contributions to the level shifts, and even for $1s - 2s$ two-photon excitation frequency there are situations where the two approaches differ in the first digit [14]. Also, as one may see in Fig. 6, there are situations where the two descriptions differ in sign. All of the data presented in this paper are in a fully relativistic framework.

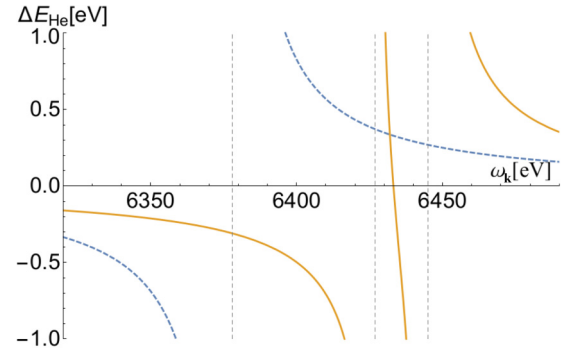


FIG. 6. Comparison of nonrelativistic (blue, dashed) and relativistic (opal, continuous) light-shift of the $1s^2$ state in He-like Fe for a laser intensity of $I = 10^{18}$ W/cm².

In Fig. 7 we have represented the light-shift for the $1s^2$ energy level in a He-like ion, for a $1s - 2s$ two-photon transition frequency, and a laser intensity of $I = 10^{18}$ W/cm² as function of the charge number Z . The M1 contribution is multiplied by 10 000. The light-shift (contribution of the electric and magnetic components of the laser) is dominated by the ac Stark shift, and for this reason in all our future analyses we neglect the magnetic contributions.

The retardation effect for $1s - 2s$ two photon excitation frequency has 1% contribution in He-like Xe and 3% contribution in He-like U. It is relevant only when the photon energy is comparable to the atomic binding energy. Anyhow, this effect was included in all our data.

For $J = 2$, the only nonzero results are for $J_v = 2$ and $j_v = \frac{3}{2}$ or $\frac{5}{2}$. In Eq. (59), the product of the two Clebsch-Gordan coefficients are nonzero in the special case $M = M_i = M_v = 0$. Note that a product of two Clebsch-Gordan coefficients is present in all situations presented in Fig. 5 and always will give the same relation between the magnetic quantum numbers, i.e., $M = M_i = M_v = 0$. In all further computations, one should consider this relation a known property of the He-like systems. Introducing in Eq. (59) the above quantities, as in the $J = 1$ case, one gets a light-shift for He-like ions 2 times the light-shift for H-like ions. However, this contribution is very small: for a $1s - 2s$ two-photon transition frequency

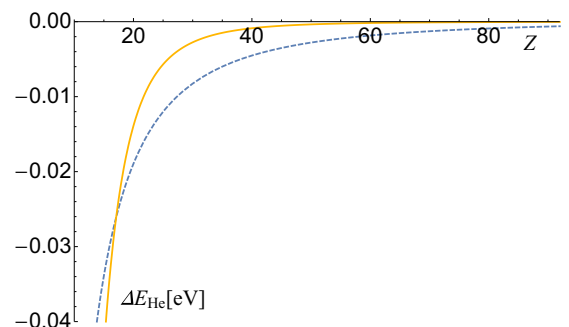


FIG. 7. Light-shift of the $1s^2$ energy level in a He-like ion, for a $1s - 2s$ two-photon transition frequency and a laser intensity of $I = 10^{18}$ W/cm² as function of the charge number Z . The E1 (blue, dashed) and $M1 \times 10^4$ (opal, continuous) contributions are shown.

TABLE I. The β coefficients (66) in $[\text{Hz}(\text{W}/\text{m}^2)^{-1}]$ for the He-like $[1s^2]_{J_i=0}$ state for different two-photon transition frequencies and for different charge states Z . $x[y]$ stands for $x \times 10^y$.

Z	$1s - 2s$	$1s - 3s$	$1s - 4s$
26	-1.11253[-10]	-1.25437[-10]	-1.32129[-10]
37	-2.56743[-11]	-2.89360[-11]	-3.04725[-11]
46	-1.01093[-11]	-1.13894[-11]	-1.19915[-11]
53	-5.41038[-12]	-6.09378[-12]	-6.41470[-12]
63	-2.44656[-12]	-2.75473[-12]	-2.89908[-12]
73	-1.19454[-12]	-1.34490[-12]	-1.41514[-12]
78	-8.50281[-13]	-9.57426[-13]	-1.00740[-12]
83	-6.10001[-13]	-6.87061[-13]	-7.22944[-13]
89	-4.11943[-13]	-4.64276[-13]	-4.88597[-13]
91	-3.61621[-13]	-4.07684[-13]	-4.29077[-13]

and a laser intensity of $10^{18} \text{ W}/\text{cm}^2$, the light-shift for He is $9.26951 \times 10^{-5} \text{ eV}$ and for He-like U is $1.80032 \times 10^{-8} \text{ eV}$.

Light-shift is quadratic in the field strength and linear in the laser's intensity I , i.e.,

$$\Delta E_{\text{He}}(i) \propto I = \frac{1}{2} \epsilon_0 c \mathcal{E}^2, \quad (65)$$

where c is the speed of light, ϵ_0 is the vacuum permittivity, and \mathcal{E} is the field strength. In order to avoid discussions over the intensity I , and for a better comparison with existing nonrelativistic data, in the following we are introducing the dynamic Stark shift coefficient β [14]:

$$\Delta E_{\text{He}}(i) \equiv h\beta I. \quad (66)$$

The Stark shift contributions for $1s - ns$, $n \in \overline{2,4}$, two-photon transition frequency are shown in Table I. It is also intuitively understandable that external field effects in general have a smaller effect if the electrons are bound by stronger central potentials. For measurements with lighter elements, the effects are more pronounced. Anyhow, in the case of U, where the binding energies exceed 10 keV, even a photon frequency of 50 eV is negligible in the description of the dynamic Stark shift. However, for lighter systems such as Xe ($Z = 54$), the difference between the optical and the soft x-ray light field is noticeable [14], especially for excited states.

TABLE II. The β coefficients (66) in $[\text{Hz}(\text{W}/\text{m}^2)^{-1}]$ for the He-like $[2p_{3/2}^2]_{J_i=0}$ state for different two-photon transition frequencies and for different charge states Z . $x[y]$ stands for $x \times 10^y$.

Z	$2p_{3/2} - 3s$	$2p_{3/2} - 4s$	$2p_{3/2} - 3p_{3/2}$
26	-4.72485[-9]	-6.23940[-9]	-4.73734[-9]
37	-1.16221[-9]	-1.51013[-9]	-1.16773[-9]
46	-4.91971[-10]	-6.27594[-10]	-4.95047[-10]
53	-2.82666[-10]	-3.54089[-10]	-2.84594[-10]
63	-1.45398[-10]	-1.76052[-10]	-1.46204[-10]
73	-8.43263[-11]	-9.72769[-11]	-8.42404[-11]
78	-6.69466[-11]	-7.46866[-11]	-6.63897[-11]
83	-5.47799[-11]	-5.84738[-11]	-5.36454[-11]
89	-4.53062[-11]	-4.47161[-11]	-4.31147[-11]
91	-4.32609[-11]	-4.11545[-11]	-4.05292[-11]

TABLE III. The β coefficients (66) in $[\text{Hz}(\text{W}/\text{m}^2)^{-1}]$ for the He-like $[1s2p_{1/2}]_{J_i=0}$ state for different two-photon transition frequencies and for different charge states Z . $x[y]$ stands for $x \times 10^y$.

Z	$1s - 2s$	$1s - 3s$	$2p_{1/2} - 2p_{3/2}$
26	-3.66886[-11]	-4.14022[-11]	-2.89356[-11]
37	-8.35255[-12]	-9.41610[-12]	-6.61010[-12]
46	-3.23837[-12]	-3.64674[-12]	-2.57232[-12]
53	-1.70702[-12]	-1.92036[-12]	-1.36060[-12]
63	-7.50995[-13]	-8.43470[-13]	-6.02045[-13]
73	-3.53701[-13]	-3.96517[-13]	-2.85452[-13]
78	-2.46256[-13]	-2.75795[-13]	-1.99470[-13]
83	-1.72205[-13]	-1.92671[-13]	-1.40027[-13]
89	-1.12145[-13]	-1.25328[-13]	-9.16290[-14]
91	-9.71010[-14]	-1.08476[-13]	-7.94665[-14]

Unfortunately, light-shifts can never be entirely eliminated in two-photon spectroscopy, because the transition between level is made by virtual transitions through intermediate states that are usually far from resonance. In this paper we give some examples of two-photon transitions for highly charged ions with an effective nuclear charge bigger than 26. Recently, the Rayleigh scattering of x rays by heliumlike Ni^{26+} ions in their ground state was studied beyond the IPM (identical particle model) [35]. The obtained results show that, for highly energetic photons, the effects beyond the IPM do not exceed 2%.

In Table V, we are giving some light-shift formulas for different electronic configurations in He-like ions. The first column in the table contains a set of possible electronic configurations, the second one the He-like light-shift as a function of H-like light-shift [14], and the last column the corresponding table with numerical data for different charge states. The list of light-shifts can be extended straightforwardly to other transitions of interest.

IV. SUMMARY

This paper is a fully relativistic, semi-QED description of the light-shifts of energy levels in highly charged ions, valid for arbitrary values of nuclear charge. We are using the

TABLE IV. The β coefficients (66) in $[\text{Hz}(\text{W}/\text{m}^2)^{-1}]$ for the He-like $[1s2p_{3/2}]_{J_i=1}$ state for different two-photon transition frequencies and for different charge states Z . $x[y]$ stands for $x \times 10^y$.

Z	$1s - 2s$	$2p_{3/2} - 3s$	$2p_{3/2} - 3p_{3/2}$
26	-1.11762[-10]	-8.89182[-11]	-8.89243[-11]
37	-2.59568[-11]	-2.06834[-11]	-2.06863[-11]
46	-1.02934[-11]	-8.21530[-12]	-8.21705[-12]
53	-5.54665[-12]	-4.43303[-12]	-4.43429[-12]
63	-2.53838[-12]	-2.03307[-12]	-2.03388[-12]
73	-1.25811[-12]	-1.00981[-12]	-1.01036[-12]
78	-9.03485[-13]	-7.25895[-13]	-7.26340[-13]
83	-6.54611[-13]	-5.26401[-13]	-5.26767[-13]
89	-4.48055[-13]	-3.60597[-13]	-3.60886[-13]
91	-3.95262[-13]	-3.18172[-13]	-3.18438[-13]

TABLE V. The He-like light-shift for different electronic configurations as a function of H-like light-shift. $\Delta E_{\text{H}}(a \rightarrow b)$ stands for the part of the light-shift corresponding to the $a - b$ transition. The last column gives the corresponding table with data.

i	$\Delta E_{\text{He}}(i)$	Table
$1s^2$	$2\Delta E_{\text{H}}(1s)$	Table I
$[2p_{3/2}^2]_{J_i=0}$	$\Delta E_{\text{H}}(2p_{3/2}; j_v = \frac{1}{2}) + 10 \Delta E_{\text{H}}(2p_{3/2}; j_v = \frac{3}{2}) + \frac{5}{3} \Delta E_{\text{H}}(2p_{3/2}; j_v = \frac{5}{2})$	Table II
$[1s2s]_{J_i=0}$	$\Delta E_{\text{H}}(1s)$	$\frac{1}{2} \times$ Table I
$[1s2p_{1/2}]_{J_i=0}$	$\Delta E_{\text{H}}(1s) - \Delta E_{\text{H}}(1s \rightarrow 2p_{1/2})$	Table III
$[1s2s]_{J_i=1}$	$3\Delta E_{\text{H}}(1s)$	$\frac{3}{2} \times$ Table I
$[1s2p_{1/2}]_{J_i=1}$	$3\Delta E_{\text{H}}(1s) - 3\Delta E_{\text{H}}(1s \rightarrow 2p_{1/2})$	$3 \times$ Table II
$[1s2p_{3/2}]_{J_i=1}$	$3\Delta E_{\text{H}}(1s) - \frac{3}{2} \Delta E_{\text{H}}(1s \rightarrow 2p_{3/2})$	Table IV

T -matrix formalism in order to develop a relativistic many-body light-shift theory. Furthermore, using the independent particle model, one may decompose the He-like matrix elements into H-like matrix elements. This allows us to relate the He-like light-shift to the H-like light-shift, and the latter is computed in literature.

In our analysis, we are expanding the electromagnetic field into multipoles which enables us to study the nondipole effects of retardation and the interaction with the magnetic components of the field. Both contributions are significant just near resonances, so the main addition to the Stark shift comes from the E1 transitions. One may conclude that the dipole approximation is good, especially for low charge states where the retardation effect is small. Also, if one compares Table I with Table II, one can see that light mainly affects the upper levels.

The theory presented in this paper is important for current and future experiments. Doppler-free two-photon spectroscopy is never free of light-shift effects. Recently, observations involving two-photon absorption in the x-ray regime have been reported at SACLA [36,37].

ACKNOWLEDGMENTS

O.P. was supported by the Strategic Grant No. POS-DRU/159/1.5/S/137750, Project Doctoral and Postdoctoral Programs, Support for Increased Competitiveness in Exact Sciences Research, cofinanced by the European Social Fund within the Sectoral Operational Program Human Resources Development 2007–2013.

-
- [1] R. Szymtkowski, *Phys. Rev. A* **65**, 012503 (2001).
- [2] J. J. Sakurai, *Modern Quantum Mechanics* (Addison-Wesley Publishing Company, Inc., Boston, MA, 1994).
- [3] B. M. Branden and C. J. Joachain, *Introduction to Quantum Mechanics* (Longman, New York, 1989).
- [4] A. Messiah, *Quantum Mechanics* (Dunod, Paris, France, 1966).
- [5] S. L. Haan and V. L. Jacobs, *Phys. Rev. A* **40**, 80 (1989).
- [6] C. Beilmann, O. Postavaru, L. H. Arntzen, R. Ginzler, C. H. Keitel, V. Mäkel, P. H. Mokler, M. C. Simon, H. Tawara, I. I. Tupitsyn, J. Ullrich, J. R. Crespo López-Urrutia, and Z. Harman, *Phys. Rev. A* **80**, 050702(R) (2009).
- [7] C. Cohen-Tannoudji, *Atoms in Electromagnetic Fields* (World Scientific Publishing Co., Singapore, 2004).
- [8] W. Rudin, *Functional Analysis* (McGraw-Hill, Inc., New York, 1991).
- [9] V. G. Gorshkov and L. N. Labzovsky, *Zh. Eksp. Teor. Fiz.* **69**, 1141 (1975).
- [10] V. M. Shabaev, A. V. Volotka, C. Kozhuharov, G. Plunien, and Th. Stöhlker, *Phys. Rev. A* **81**, 052102 (2010).
- [11] A. Schäfer, G. Soff, P. Indelicato, B. Müller, and W. Greiner, *Phys. Rev. A* **40**, 7362 (1989).
- [12] POLARIS-Jena, <https://polaris-jena.de/>.
- [13] PHELIX-GSI, <https://www.gsi.de/phelix>.
- [14] O. Postavaru, Ph.D. thesis, Heidelberg University, Germany, 2010.
- [15] A. Surzhykov, P. Indelicato, J. P. Santos, P. Amaro, and S. Fritzsche, *Phys. Rev. A* **84**, 022511 (2011).
- [16] P. J. Mohr, G. Plunien, and G. Soff, *Phys. Rep.* **293**, 227 (1998).
- [17] O. Yu. Andreev, L. N. Labzovsky, G. Plunien, and D. A. Solov'ev, *Phys. Rep.* **455**, 135 (2008).
- [18] V. M. Shabaev, *Phys. Rep.* **356**, 119 (2002).
- [19] I. Lindgren, S. Salomonson, and B. Åsén, *Phys. Rep.* **389**, 161 (2004).
- [20] M. I. Mishchenko, G. Videen, V. A. Babenko, N. G. Khlebtsov, and Th. Wriedt, *J. Quant. Spectrosc. Radiat. Transfer* **88**, 357 (2004).
- [21] P. C. Waterman, *Proc. IEEE* **53**, 805 (1965).
- [22] W. R. Johnson and G. Soff, *At. Data Nucl. Data Tables* **33**, 405 (1985).
- [23] W. R. Johnson, *Atomic Structure Theory – Lectures on Atomic Physics* (Springer, New York, 2007).
- [24] W. Greiner, *Relativistic Quantum Mechanics* (Springer, New York, 1997).
- [25] H. Feshbach, *Ann. Phys. (NY)* **19**, 287 (1962).
- [26] H. Feshbach, *Ann. Phys. (NY)* **5**, 357 (1958).
- [27] R. Gamkrelidze, *Theory of Operators* (Consultants Bureau, New York, 1991).
- [28] S. Zakowicz, Ph.D. thesis, Justus-Liebig of Gießen, Germany, 2001.
- [29] J. J. Sakurai, *Modern Quantum Mechanics* (Addison-Wesley Publishing Company, Reading, MA, 1994).
- [30] M. Haas, U. D. Jentschura, and C. H. Keitel, *Am. J. Phys.* **74**, 77 (2006).

- [31] A. S. Kheifets, A. W. Bray, and I. Bray, *Phys. Rev. Lett.* **117**, 143202 (2016).
- [32] M. Abramowitz and I. A. Stegun, *Handbook of Mathematical Functions* (National Bureau of Standards, Gaithersburg, MD, 1972).
- [33] D. M. Brink and G. R. Satchler, *Angular Momentum* (Oxford Science Publications, Oxford, UK, 2002).
- [34] R. Szmytkowski, *J. Phys. B: At., Mol. Opt. Phys.* **30**, 825 (1997).
- [35] A. V. Volotka, V. A. Yerokhin, A. Surzhykov, Th. Stöhlker, and S. Fritzsche, *Phys. Rev. A* **93**, 023418 (2016).
- [36] K. Tamasaku, E. Shigemasa, Y. Inubushi, T. Katayama, K. Sawada, H. Yumoto, H. Ohashi, H. Mimura, M. Yabashi, K. Yamauchi, and T. Ishikawa, *Nat. Photonics* **8**, 313 (2014).
- [37] S. Ghimire, M. Fuchs, J. Hastings, S. C. Herrmann, Y. Inubushi, J. Pines, S. Shwartz, M. Yabashi, and D. A. Reis, *Phys. Rev. A* **94**, 043418 (2016).